Available online at www.sciencedirect.com
SCIENCE DIRECT®
Journal of Solid State Chemistry 178 (2005) 36–40
JOURNAL OF SOLID STATE CHEMISTRY
www.elsevier.com/locate/jssc

The structure, photo-induced magnetization and correlation of the cyano-bridged two-dimensional hetero-bimetallic compounds

Guangming Li[a,b], Pengfei Yan[b], Osamu Sato[c], Yasuaki Einaga[a,*]

[a]*Department of Chemistry, Faculty of Science and Technology, Keio University, 3-14-1 Hiyoshi, Yokohama-shi, Kanagawa-ken 223-8522, Japan*
[b]*Faculty of Chemistry and Material Science, Heilongjiang University, 74 Xuefu Road, Nangang District, Harbin 150080, P.R. China*
[c]*Kanagawa Academy of Science and Technology, KSP Building East 412, 3-2-1 Sakado, Kawasaki 213-0012, Japan*

Received 30 August 2004; accepted 14 October 2004

Abstract

Two new 3*d*–4*f* cyano-bridged hetero-bimetallic compounds with distinguished two-dimensional honeycomb network structure, $\{Ln(HP)_2(H_2O)_3(\mu\text{-}NC)_3Fe(CN)_3\}_n$, (*Ln* = Ce, Nd; HP = 4-Hydroxypyridine) were synthesized and crystallographically characterized. A novel photo-induced magnetization phenomenon for $\{Nd(HP)_2(H_2O)_3(\mu\text{-}NC)_3Fe(CN)_3\}_n$, was revealed and studied. Furthermore, the correlation between photo-induced magnetization and structure was proposed.

Keywords: Lanthanide metal; Iron; Cyano-bridged; Crystal structure; Photo-induced magnetization

1. Introduction

The photo-induced magnetization and corresponding mechanism for Prussian blue analogues and other transition metal compounds have been studied in the past decade [1–5]. It is proposed that the photo-induced magnetization change by light irradiation derived from electron transfer and/or electron polarization. This is accompanied with a structure deformation that has to taken up by the flexible inorganic network via the vacancies, hydrogen bonds and $\pi-\pi$ interactions. Thus, an introduction of a flexible network structure in the crystals is essential for originating a photo-induced magnetization [3b,4c]. On the basis of such a strategy, the photo-induced magnetization of the cyano-bridged 3*d*−4*f* hetero-bimetallic assembly $[Nd(DMF)_4(H_2O)_3(\mu\text{-}NC)Fe(CN)_5]\cdot H_2O$ (DMF = *N*,*N*-dimethylformamide) (**1**) [6] and $[Nd(DMF)_4(H_2O)_3(\mu\text{-}NC)Co(CN)_5]\cdot H_2O$ (**2**) [7] has been reported. To further explore this interesting photo-induced magnetization phenomenon and the correlation between the photo-induced magnetization and structures, two new cyano-bridged 3*d*–4*f* hetero-bimetallic assembly $\{Ln(HP)_2(H_2O)_3(\mu\text{-}NC)_3Fe(CN)_3\}_n$ (*Ln* = Nd (**3**) and Ce (**4**), HP = 4-Hydroxypyridine) have been designed, synthesized and structurally characterized. As a result, a weakened photo-induced magnetization change of **3** was observed. Further studies revealed the correlation between the structure and the photo-induced magnetization.

2. Experimental

2.1. General procedures

All chemicals and solvents of commercial grade were used as purchased without further purification. UV light irradiation was conducted using an ultra-high-pressure mercury lamp (HYPERCURE 200, Yamashita Denso). Low temperature was achieved by using a variable-temperature cryostat and monitored by a thermocouple together with the variable-temperature cryostat for IR spectra. Elemental analysis was carried out on an

*Corresponding author. Fax: +81 45 566 1697.
E-mail address: einaga@chem.keio.ac.jp (Y. Einaga).

0022-4596/$ - see front matter © 2004 Elsevier Inc. All rights reserved.
doi:10.1016/j.jssc.2004.10.027

Elementar Vario EL at the Central Facilities for Science and Technology Research, Keio University. Infrared (IR) spectra were recorded by KBr discs on a BIO-RAD FTS-165 FTIR spectrometer over the range of 400–4000 cm^{-1}. Magnetic properties were investigated with a superconducting quantum interference device (SQUID) magnetometer (Quantum Design MPMS-5S).

2.2. Synthesis of $\{Ln(HP)_2(H_2O)_3(\mu\text{-}NC)_3Fe(CN)_3\}_n$ (Ln=Nd (3) and Ce (4), HP=4-Hydroxypyridine)

3 & **4** were synthesized by the facile reactions of $LnCl_3 \cdot 6H_2O$ (1.0 mmol) in water (10 mL), HP (2.0 mmol) in ethanol (5 mL), and $K_3[Fe(CN)_6]$ (1.0 mmol) in water (10 mL) in a 30 mL glass test tube of 15 mm diameter. The red crystals were harvested by layering the mixture of $LnCl_3 \cdot 6H_2O$ and HP on the top of the aqueous solution of $K_3[Fe(CN)_6]$ for 1–2 days. For **3**: orange-red crystals. Yield: 60%. Anal. Calcd for $C_{16}H_{16}FeN_8NdO_5$ (%) (**3**): C, 32.01; H, 2.69; N, 18.66; found C, 32.23; H, 2.46; N, 18.35. For **4**: brown crystals. Yield: 65%. Anal. Calcd for $C_{16}H_{16}FeN_8FeO_5$ (%) (**4**): C, 32.23; H, 2.70; N, 18.79; found C, 32.48; H, 2.51; N, 18.56.

2.3. Crystallographic studies

The crystals of **4** used for analysis were mounted on the top of a glass capillary and wrapped with Vaseline to prevent the loss of co-crystallized solvent molecules. Data collection was carried out on an *RAPID-AUTO* imaging plate system using graphite-monochromatized Mo*K* radiation ($\lambda = 0.71073$ Å). The determination of crystal class, orientation matrix and cell dimensions was performed according to established procedures. All data processing was performed with the *SHELXS*97 program package [8]. Analytical expressions of neutral-atom scattering facts were employed and anomalous dispersion corrections were incorporated. The raw data were processed with the learnt-profile procedure, and absorption corrections were applied using an algorithm that was based on the correction of equivalent reflections. The positions of all hydrogen atoms were generated geometrically (C–H bonds fixed at 0.096 Å), assigned isotropic thermal parameters and allowed to ride on their respective parent C atoms. Crystal data, data collection parameters and the results of the analysis are listed in Table 1.

Table 1
Crystallographic data for $\{Ce(HP)_2(H_2O)_3(\mu\text{-}NC)_3Fe(CN)_3\}_n$, **4**

Empirical formula	$C_{16}H_{16}CeFeN_8O_5$
Formula weight	596.34
Temperature	293(2) K
Wavelength	0.71073 A
Crystal system, space group	Monoclinic, $P2(1)/m$
Unit cell dimensions	$a = 7.0513(14)$ Å, $\alpha = 90°$ $b = 15.903(3)$ Å, $\beta = 101.96(3)°$ $c = 9.862(2)$ Å, $\gamma = 90°$
Volume	1081.9(4) A^3
Z; calculated density	2; 1.831 Mg/m^3
Absorption coefficient	2.792 mm^{-1}
$F(000)$	584
Crystal size	0.52 × 0.34 × 0.28 mm
Theta range for data collection	3.22–27.48°
Limiting indices	$-9 \leqslant h \leqslant 9$, $-20 \leqslant k \leqslant 20$, $-12 \leqslant l \leqslant 12$
Reflections collected/unique	10433/2561 [$R_{int} = 0.0508$]
Completeness to $\theta = 27.48$	99.80%
Absorption correction	Semi-empirical from equivalents
Max. and min. transmission	0.5086 and 0.3246
Refinement method	Full-matrix least-squares on F^2
Data/restraints/parameters	2561/6/167
Goodness-of-fit on F^2	1.084
Final R indices [$I > 2\sigma(I)$]	$R_1 = 0.0541$, w$R_2 = 0.1536$
R indices (all data)	$R_1 = 0.0552$, w$R_2 = 0.1545$
Largest diff. peak and hole	4.381 and −1.161 e A^{-3}

3. Results and discussion

3.1. Photo-induced magnetization

To study photo-induced magnetization change of **3**, a UV lamp was used as the light source. The UV light was transmitted through an optical fiber into the SQUID magnetometer for illumination of the sample. Upon irradiation at 5 K, the magnetization was slightly increased and gradually saturated after several hours. The plot of $\chi_M T$ versus T for **3** (Fig. 1) has clearly shown that the $\chi_M T$ values were enhanced as compared to those before irradiation in the temperature range of 5–12 K. By increasing the temperature to 12 K, the photo-induced magnetization was erased. This indicated that the photo-excited state had reached to the ground state.

Notice that (1) the photo-excited state remained stable below the decay temperature. However, it relaxed back to the ground state when the temperature reached the decay temperature. Therefore it is difficult obtaining the decay curve or relaxation curve; (2) the scale of the photo-induced magnetization change for **1**, **2** and **3** is much smaller as compared to that for Prussian blue's. In the former, they are still in a range of para-magnetization although the $\chi_M T$ values were enhanced by about 45% after light irradiation. However, the para-magnetization turned to ferri-magnetization in the latter after light irradiation; (3) the $\chi_M T$ herein are relative values but not absolute and the change of photo-induced magnetization depended on the sample geometry and the light transmission.

In our previous report, the significant photo-induced magnetization change of the cyano-bridged 3*d*–4*f* hetero-bimetallic assembly **1** and **2** had been described in which the $\chi_M T$ values were significantly enhanced by

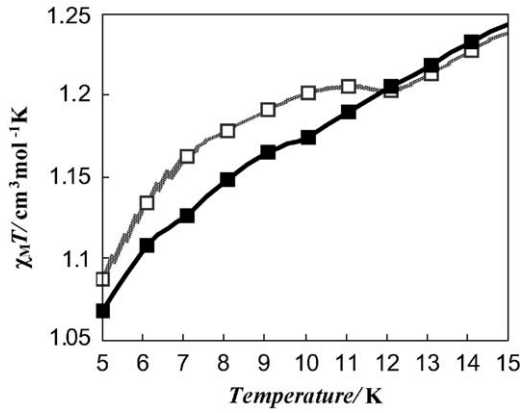

Fig. 1. Plots of magnetic susceptibilities ($\chi_M T$) versus temperature (T) for **3** at $H = 5000$ G: Before (■) and after (□) UV light illumination.

UV and visible light illumination [6,7]. The recovery temperature was 50 and 40 K, respectively. The mechanism of photo-induced magnetization was also discussed [6,7,9–11]. It was proposed that UV light illumination induced a LMCT transition, accompanied with an increase in the electron population on Fe(III) ion. This was followed by an increment in the ligand–metal bond length and a small structural change in the inorganic network. The small structural change was propagated by molecular interaction in the inorganic network. Further, the cooperativity resulted from the molecular interaction served to increase the activation energy of the relaxation process, which resulted in the observation of the photo-excited state. It was this cooperativity arisen from the flexible network that led to the photo-induced magnetization change.

Because the compositions of **1**, **2** and **3** are closed related, we propose that the mechanism of the photo-induced magnetization should be the same. However, when compared to **1** and **2**, the photo-induced magnetization for **3** was observed to have significantly weakened.

3.2. Structural analysis

To explain these significant differences between them, single crystal structural and other spectroscopic analysis have been carried out. Single-crystal structural analysis have proposed that $\{Ce(HP)_2(H_2O)_3(\mu\text{-}NC)_3Fe(CN)_3\}_n$ (**4**) crystallized in a monoclinic system with space group $P2_1/m$ and $Z = 2$ (Table 1). The Fe(III) ions afforded a six-coordinated distorted octahedral geometry (approximately O_h symmetry, Figs. 2 and 3) coordinated by six cyanide ligands. The distances of Fe–C are in the range from 1.905(8) to 1.957(9) Å. The Ce(III) ions took an eight-coordinated distorted square antiprism coordination geometry (approximately D_{4d} symmetry) surrounded by two oxygen atoms from HP (the distances of Ce–O are 2.358(5) Å), three oxygen atoms from waters (the distances of Ce–O are in the range of 2.493(5) and 2.587(7) Å), and three cyanides from $[Fe(CN)_6]^{3-}$ moiety (the distances of Ce–N are in the range from 2.629(8) to 2.678(7) Å). The angle of Ce–N–C is 145.7(8)° which is significantly different from 180°.

The important bond distances and angles showed that they are consistent with those of close-related compounds $[Ce(DMF)_4(H_2O)_3(\mu\text{-}NC)M(CN)_5]\cdot H_2O$ (M = Fe and Co, DMF = *N*,*N*-dimethylformamide) [12]. However, the angles of Ce–N–C are essentially reduced from about 175° to 145° on the basis of comparison between **3** and compounds $[Ce(DMF)_4(H_2O)_3(\mu\text{-}NC)M(CN)_5]\cdot H_2O$ (M = Fe and Co, DMF = *N*,*N*-dimethylformamide) [13]. This is derived from the six-sided ring tension of $Ce_4Fe_4(CN)_6$. Interestingly, the similar six-sided $Nd_4Fe_4(CN)_8$ rings were observed in compounds $[NdM(bpym)(H_2O)_4(CN)_6]\cdot 3H_2O$ (M = Fe, Co, *bpym* = 2,2′-bipyrimidine) [14]. Obviously, the number of CN are different in the former and latter. Therefore, a two-dimensional distorted honeycomb structure has essentially formed via three cyanide bridges (Fig. 3). This is distinguished from their DMF analogues. It should be noted that the weak coordination HP ligand played a critical role in forming such a structure.

Unfortunately, the crystal structure of **3** was not solved due to the poor quality of the crystals. However, the signal crystal structure of **4**, which is an isomorphous crystal to **3** based on the microanalysis and spectroscopic analysis, has been determined. Namely, **3** should take the same rigid two-dimensional honeycomb network structure as **4**. In contrast, **1** [6] and **2** [13] adopted a flexible three-dimensional network structure via hydrogen bonds.

3.3. Correlation of the structure and photo-induced magnetization

The above-mentioned crystallographic analysis showed that **3** took a rigid two-dimensional honeycomb network structure. It is different from the flexible network structures of **1** and **2**. On the basis of the differences of photoinduced magnetization changes among **1**, **2** and **3**, the photo-induced magnetization is correlated to the structures of the compounds. Namely, it is this rigid network structure that dominates the weakened photo-induced magnetization of **3**. Because the steric strains in a rigid network structure were strong that only the molecules at the surface of the bulk for **3** were excited, while the other molecules in the bulk were not. Specially, the propagation of the photo-excited state was hindered in the bulk, which resulted in the weakened photo-induced magnetization of **3**. On the contrary, the steric strains in a flexible structure are weaker than those in a rigid structure, as such, a

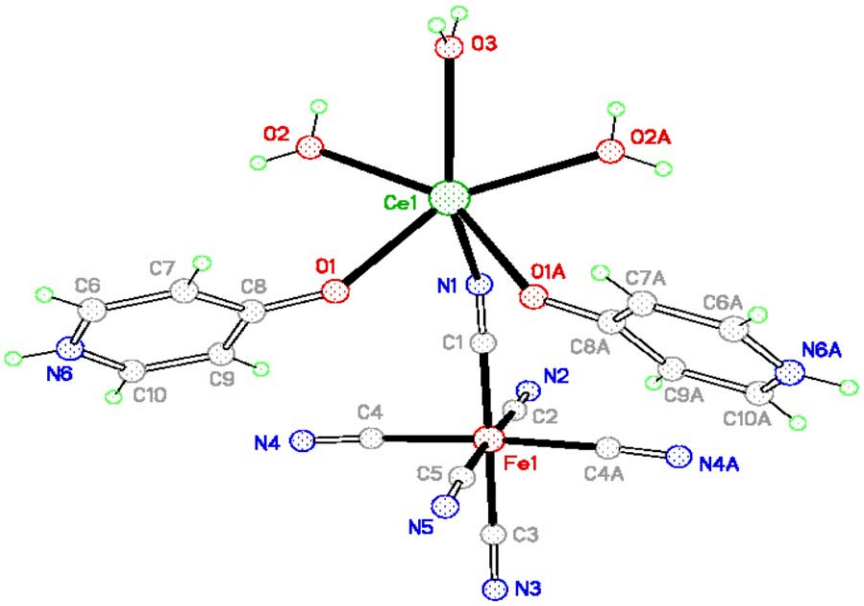

Fig. 2. A view of the molecular structure for **4**: Hydrogen atoms are omitted for clarity and the thermal ellipsoids are drawn at 50% probability level. Selected bond distances (Å) and angles (deg): Ce(1)–O(1) 2.358(5); Ce(1)–O(1)A 2.358(5); Ce(1)–O(2)A 2.493(5); Ce(1)–O(2) 2.493(5); Ce(1)–O(3) 2.587(7); Ce(1)–N(1) 2.645(7); Fe(1)–C(5) 1.905(8); Fe(1)–C(4) 1.937(6); Fe(1)–C(4)A 1.937(6); Fe(1)–C(1) 1.946(8); Fe(1)–C(3) 1.954(8); Fe(1)–C(2) 1.957(9); N(1)–C(1) 1.164(11); N(2)–C(2) 1.125(11); N(3)–C(3) 1.124(12); N(4)–C(4) 1.142(9); N(5)–C(5) 1.125(12); N(6)–C(6) 1.313(15); N(6)–C(10) 1.340(15); C(8)–O(1)–Ce(1) 149.7(5); C(1)–N(1)–Ce(1) 145.7(8); N(1)–C(1)–Fe(1) 178.9(7); N(2)–C(2)–Fe(1) 176.2(9); N(3)–C(3)–Fe(1) 176.7(8); N(4)–C(4)–Fe(1) 176.6(6); N(5)–C(5)–Fe(1) 175.1(8).

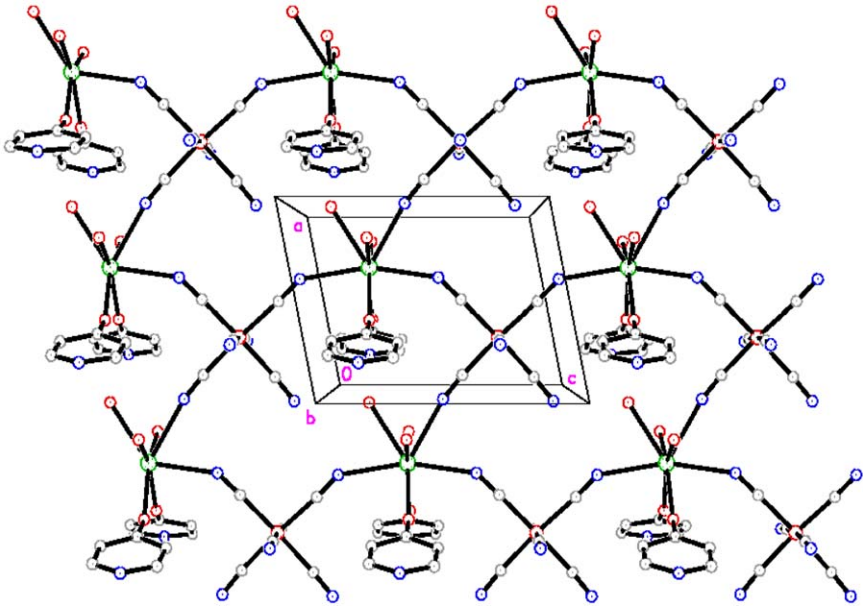

Fig. 3. The two-dimensional network packing structure of **4**.

photo-induced metastable state could be propagated in the bulk [3b,6]. Adding further support to this proposal, the IR spectra for **3** were conducted at 8 K before and after UV light illumination (Fig. 4). Interestingly, the wide peak around 2050 cm^{-1} rapidly saturated after UV light illumination, which showed that the change was much lesser than that of **1** and **2**. It indicated that the photo-induced structural distortion was significantly hindered by steric strains. In addition, UV spectra for **3** (not shown) revealed a small change in terms of the LMCT band around 430 cm^{-1} at 8 K as compared to **1** after UV light irradiation. However, the quantitative discussion on the spectra was difficult.

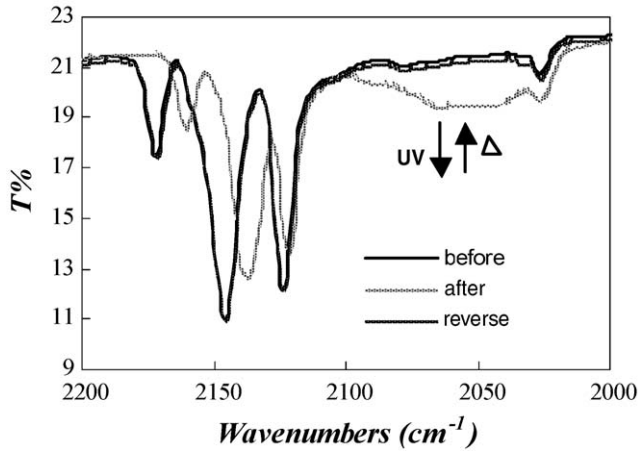

Fig. 4. IR spectra (KBr pallet) for **3** at 8 K: before (solid line) and after (dotted line) UV light illumination, and annealing (dashed line).

In summary, two new cyan-bridged hetero-bimetallic compounds with distinguished two-dimensional structure have been synthesized, characterized as well as the corresponding photo-induced magnetic phenomenon for **3** were observed and described, however, the photo-induced magnetization was diminished as compared to that of **1** and **2**. Further studies revealed that the weakened photo-induced magnetization is derived from the rigid network structure of **3**. Therefore, besides the findings of the new compounds with novel photo-induced magnetization, this work, to our knowledge, has provided the first experimental evidence that the propagation of photo-excited state could be obstructed by the steric strains arisen in the rigid network. This demonstration is not only applicable for the photo-induced magnetic phenomena but also can be used for a variety of other photo-induced phenomena, such as photo-induced spin transition, etc.

Acknowledgments

This work is supported by Grant-in-Aid for Scientific Research on Priority Areas (417) and for the 21st century COE program "Keio Life Conjugate Chemistry" from the Ministry of Education, Culture, Sport, Science, and Technology (MEXT) of Japan.

References

[1] (a) P. Gütlich, Y. Garcia, T. Woike, Coord. Chem. Rev. 219–221 (2001) 838–879;
(b) P. Gütlich, A. Hauser, H. Spiering, Angew. Chem. Int. Ed. Engl. 33 (1994) 2024–2054.
[2] (a) D.A. Pejakovic, J.L. Manson, J.S. Miller, A.J. Epstein, J. Appl. Phys. 87 (2000) 6028–6030;
(b) D.A. Pejakovic, J.L. Manson, J.S. Miller, A.J. Epstein, Phys. Rev. Lett. 85 (2000) 1994–1997.
[3] (a) A. Bleuzen, C. Lomenech, V. Escax, F. Villain, F. Varret, C.C.D. Moulin, M. Verdaguer, J. Am. Chem. Soc. 122 (2000) 6648–6652;
(b) C. Cartier, F. Villain, A. Bleuzen, M.-A. Arrio, P. Sainctavit, C. Lomenech, V. Escax, F. Baudelet, E. Dartyge, J.-J. Gallet, M. Verdaguer, J. Am. Chem. Soc. 122 (2000) 6653–6658.
[4] (a) O. Sato, T. Iyoda, A. Fujishima, K. Hashimato, Science 272 (1996) 704–705;
(b) O. Sato, Y. Einaga, A. Fujishima, K. Hashimato, Inorg. Chem. 38 (1999) 4405–4412;
(c) O. Sato, S. Hayami, Y. Einaga, Z.-Z. Gu, Bull. Chem. Soc. Jpn. 76 (2003) 443–470.
[5] (a) S. Ohkoshi, A. Fujishima, K. Hashimoto, J. Am. Chem. Soc. 120 (1998) 5349–5350;
(b) S. Ohkoshi, K. Hashimoto, J. Am. Chem. Soc. 121 (1999) 10591–10597;
(c) S. Ohkoshi, Y. Einaga, A. Fujishima, K. Hashimoto, J. Electroanal. Chem. 473 (1999) 245–249.
[6] G. Li, T. Akitsu, O. Sato, Y. Einaga, J. Am. Chem. Soc. 125 (2003) 12396–12397.
[7] G. Li, O. Sato, T. Akitsu, Y. Einaga, J. Solid State Chem. 177 (2004) 3835–3838.
[8] G.M. Sheldrick, SHELXS97 and SHELXL97, University of Göttingen, Germany, 1997.
[9] S. Hayami, Z.-Z. Gu, M. Shiro, Y. Einaga, A. Fujishima, O. Sato, J. Am. Chem. Soc. 122 (2000) 7126–7127.
[10] M. Marchivie, P. Guionneau, J.A.K. Howard, G. Chastanet, J.-F. Letard, A.E. Goeta, D. Chasseau, J. Am. Chem. Soc. 124 (2002) 194–195.
[11] T. Wojtowicz, S. Kolesnik, I. Miotkowski, J.K. Furdyna, Phys. Rev. Lett. 70 (1993) 2317–2320.
[12] A. Figuerola, C. Diaz, J. Ribas, V. Tangoulis, J. Granell, F. Lloret, J. Mahia, M. Maestro, Inorg. Chem. 42 (2003) 641–649.
[13] G. Li, T. Akitus, O. Sato, Y. Einaga, J. Coord. Chem. 57 (2004) 189–198.
[14] B.-Q. Ma, S. gao, G. Su, G.-X. Xu, Angew. Chem. Int. Ed. 40 (2001) 434–436.